

TITLE PAGE

Influence of sympathetic activation on myocardial contractility measured with ballistocardiography and seismocardiography during sustained end-expiratory apnea.

Ballistocardiography, seismocardiography and sympathetic nerve activity

Sofia Morra, MD¹, Anais Gauthey MD², Amin Hossein MSc³, Jérémy Rabineau MSc³, Judith Racape, PhD⁵, Damien Gorlier MSc³, Pierre-François Migeotte, MSc, PhD³, Jean Benoit le Polain de Waroux, MD, PhD⁴, Philippe van de Borne MD, PhD¹

¹Department of Cardiology, Erasme hospital, Université Libre de Bruxelles, Belgium

² Department of Cardiology, Saint-Luc hospital, Université Catholique de Louvain, Belgium

³LPHYS, Université Libre de Bruxelles, Belgium

⁴ Department of Cardiology, Sint-Jan, Hospital Bruges, Bruges, Belgium

⁵ Research centre in epidemiology, biostatistics and clinical research. School of Public Health. Université libre de Bruxelles (ULB), Brussels, Belgium

41
42
43
44
45
46
47
48
49
50
51
52
53
54
55
56
57
58
59
60
61
62
63
64
65

NOTE AND NOTEWORTHY

Ballistocardiography (BCG) and seismocardiography (SCG) assess vibrations produced by cardiac contraction and blood flow, respectively, through micro-accelerometers and micro-gyroscopes. Kinetic energies (KE), and their temporal integrals (iK) during a single heartbeat are computed from the BCG and SCG waveforms in a linear and a rotational dimension. When compared to normal breathing, during an end-expiratory voluntary apnea, iK increased and was positively related to sympathetic nerve traffic rise assessed by microneurography. Further studies are needed to determine if BCG and SCG can probe sympathetic nerve changes in patients with sleep disturbances.

ABSTRACT

Background

Ballistocardiography (BCG) and seismocardiography (SCG) assess vibrations produced by cardiac contraction and blood flow, respectively, through micro-accelerometers and micro-gyroscopes. BCG and SCG kinetic energies (KE), and their temporal integrals (*i*K) during a single heartbeat are computed in linear and rotational dimensions.

Aims

To test the hypothesis that *i*K from BCG and SCG are related to sympathetic activation during maximal voluntary end-expiratory apnea.

Methods

Multiunit muscle sympathetic nerve traffic (BF, burst frequency; tMSNA, total muscular sympathetic nerve activity) was measured by microneurography during normal breathing and apnea (n=28, healthy men). *i*K of BCG and SCG were simultaneously recorded in the linear and rotational dimension, along with oxygen saturation (SatO₂) and systolic-blood pressure (SBP).

Results

The mean duration of apneas was 25.4 ± 9.4 s. SBP, BF, tMSNA increased during the apnea compared to baseline ($p = 0.01$, $p = 0.002$, $p = 0.001$, respectively), while SatO₂ decreased ($p = 0.02$). At the end of the apnea compared to normal breathing, changes of *i*K computed from BCG were related to changes of tMSNA and BF only in the linear dimension ($r = 0.85$, $p < 0.0001$; $r = 0.72$, $p = 0.002$, respectively), while changes of linear *i*K of SCG were related only to changes of tMSNA ($r = 0.62$, $p = 0.01$).

Conclusions

Maximal end expiratory apnea increases cardiac kinetic energy computed from BCG and SCG, along with sympathetic activity. The novelty of the present investigation is that linear *i*K of BCG is directly and more strongly related to the rise in sympathetic activity than the SCG, mainly at the end of a sustained apnea, likely because the BCG is more affected by the sympathetic and hemodynamic effects of breathing cessation. BCG and SCG may prove useful to assess sympathetic nerve changes in patients with sleep disturbances.

105 **INTRODUCTION**

106 The heart is one among many effector organs of the autonomic nervous system (ANS) and is
107 innervated by both divisions of the ANS, that is, the sympathetic and parasympathetic fibers,
108 which have antagonistic effects (66). Indeed, activation of the sympathetic division increases heart
109 rate (chronotropic effect), enhances myocardial contractility (inotropic effect), hasten electrical
110 conduction velocity (dromotropic effect) and hastens myocardial relaxation (lusitropic effect)
111 while the opposite happens under parasympathetic stimulation, except for myocardial
112 contractility (14, 23). Blood vessels are innervated exclusively by the sympathetic division, which
113 regulates the diameters of arterioles thus orchestrating continuously blood pressure fluctuations
114 around a homeostatic value (66). The complex interplay between the sympathetic and
115 parasympathetic nervous systems (SNS and PNS, respectively), creates a balance with the final
116 aim to guarantee the homeostasis of cardiovascular system in response to internal and external
117 stressors.

118 Variations of pH, pO₂, pCO₂, fluctuations in blood pressure modulate the activity of SNS/PNS
119 balance via a complex system of arc reflexes (14, 21, 24). Hypoxemia (24, 29, 45, 46, 55, 69),
120 hypercapnia (24, 39, 55, 69), decreased systemic blood pressure (21) are all powerful triggers of
121 SNS activation in healthy organisms. As an example, chronic exposure to intermittent hypoxia
122 (IH), as in sleep disorders breathing (SDB), is accompanied to a sustained activation of the SNS,
123 with several cardiovascular consequences (41). Voluntary breath holding also raises sympathetic
124 nerve activity (11, 24, 47, 51, 63).

125 Ballistocardiography (BCG) and seismocardiography (SCG) record the micro vibrations produced
126 rhythmically by the velocities and accelerations of the body's center of mass and cardiac muscle
127 contraction, respectively, with micro-accelerometers and gyroscopes placed on the body surface
128 (16, 18, 22, 52, 58). Modern BCG and SCG can measure linear and rotational velocities and
129 accelerations of blood stream using linear and rotational channels, respectively, and in three
130 cardinal axes using three-axial sensors (*x*: latero-lateral axis; *y*: caudo-cranial axis; *z*: antero-

131 posterior axis) (18, 31). Additionally, from the BCG and SCG waveforms, linear and rotational
132 kinetic energy (K), its temporal integral (iK), maximal power (P_{Max}), maximal displacements
133 (D_{Max}) and maximal velocities (V_{Max}) can be computed for each contractile cycle using specific
134 algorithms based on Newtonian equations (18). A growing number of evidences provide the
135 signals recorded with BCG and SCG as good indicators of myocardial function and dysfunction.
136 Metrics of iK and P_{Max} of BCG and SCG signals are well correlated to stroke volume (SV), cardiac
137 output (CO) (18, 20) and the LVEF (35); the peak of maximum energy obtained from BCG
138 waveforms well represents myocardial contractility expressed as dP/dt_{max} in animal models (6);
139 BCG and SCG signals provide information about myocardial dysfunction after acute coronary
140 syndrome (9, 36) and can assess the clinical status of patients with heart failure (19).
141 Respiration profoundly influences the amplitude of BCG and SCG waveforms (8, 33, 34, 44, 53):
142 the iK computed while deeply inspiring against an external resistance is higher than the one
143 observed while breathing normally (33). Moreover, in healthy individuals, the iK computed with
144 BCG and SCG increases progressively from the beginning to the end of a 10 seconds apnea, and
145 remain increased thereafter (34). As explained above, several factors occurring during an apneic
146 episode can trigger the SNS. The increased cardiac iK occurring during an end expiratory
147 voluntary apnea as observed in our previous investigation (34) may be secondary to SNS
148 activation. This is the hypothesis we wish to test with the present investigation: in healthy
149 individuals, the increased cardiac iK registered during a sustained end-expiratory apnea is related
150 to the activation of SNS directed to muscle blood vessels. In this study, sympathetic nerve traffic
151 was assessed directly by means of the microneurographic technique (muscle sympathetic nerve
152 activity, MSNA).

153 **METHODS**

154 *1.1 Study protocol and study population*

155 This observational study was approved by the local Ethic Committee of the Erasme hospital
156 (P201904_097) and complies with the Declaration of Helsinki. Each volunteer was asked to
157 perform regularly a sustained end-expiratory apnea, for as long as tolerated (ranging from a
158 minimum of 13s to a maximum of 49s). Each volunteer performed at least three apneas (average
159 3.8) and only one apnea per volunteer was selected based on the quality of the MSNA neurogram,
160 which was visually inspected with great care by a trained operator. Each apnea was selected
161 *prospectively* and prior to any *iK* computation. It is known that identification of bursts in a
162 neurogram is a subjective process, but standards exist to make the procedure less subjective, as
163 extensively explained by White D. and colleagues (67) and to these standards for burst
164 identification authors complied.

165 The aim of this maneuver was to induce modification of blood gases concentration to
166 activate the MSNA in order to record BCG and SCG signals simultaneously to the MSNA.

167 Twenty-eight healthy young man of 28 ± 3.6 years were enrolled.

168 None had any cardiovascular disease, took medications or drugs. The day before the experimental
169 procedure, the participant was asked not to smoke, nor drink coffee/the. Additionally, subjects
170 had to empty their bladder before the beginning of the session. Only male subjects were enrolled,
171 to avoid possible confounding effects of the menstrual cycle on the measurements.

172 Ten records were excluded from final analysis because of poor MSNA signal quality and 2 out of
173 18 remaining records had to be further excluded because of poor BCG and SCG quality signal.

174 Sixteen records were retained for final analysis.

175

176 *1.2 Experimental procedure*

177 The microneurography technique assesses multiunit postganglionic efferent sympathetic
178 activity continuously using a tungsten microelectrode (59, 67). In brief, this requires two tungsten
179 electrodes (200 μ m of shaft diameter, tapering to an uninsulated tip of 1 to 5 μ m of diameter,
180 UNA35F2S, FHC Neural MicroTargeting™), one of which is inserted in the peroneal nerve
181 proximal to the fibular head of the right leg (active electrode) (67), while the second electrode
182 (reference electrode) is placed in the subcutaneous tissue, 2-3cm away from the nerve, as
183 previously described (62-65). These signal were send to an amplifier, signal integrator and filter
184 (Nerve Traffic Analyzer; University of Iowa Bioengineering, Iowa City) (67) connected to the
185 acquisition system PowerLab 16/30 (ADInstrument).

186 One-lead ECG, systemic blood pressure, oxygen saturation (SatO₂), endtidalCO₂, were
187 continuously recorded.

188 Finger blood pressure was obtained continuously throughout the experimental session by
189 placing a cuff on the second finger of the right hand and through the use of a beat-by-beat
190 hemodynamic monitoring system (Finometer Pro, FMS®, Amsterdam, the Netherlands), allowing a
191 reliable reconstruction of the humeral blood pressure. Reconstruction of systolic, diastolic and
192 mean humeral blood pressure from Finometer® is as a reliable measurement of systemic blood
193 pressure as invasive measurements are, complying with the American Association of Medical
194 Instrumentation (AAMI) requirements, as previously reported (15).

195 A continuous one-lead ECG (ADInstruments) was obtained throughout the whole session.

196 Oxygen saturation was obtained throughout the session by placing a pulse oximeter on the second
197 finger of the left hand, while endtidal CO₂ was obtained continuously by nasal cannula
198 (Capnostream-35-monitor®, Oridion Medical 272 Ltd, Jerusalem, Israël).

199 Respiratory movements were monitored via a respiratory belt placed around the thoraco-
200 abdominal circumference (ADInstruments).

201 Signals were connected, acquired and processed with the data acquisition system PowerLab 16/30
202 and LabChart version 8.0 (ADInstruments).

203 BCG and SCG were acquired by a portable device with two detectors, one of which was a box
204 of dimension 64cm² and weight 104g placed on the manubrium of the sternum below the clavicle
205 over the superior mediastinum where the great vessels emerge from the cardiac muscle. The
206 second detector was a box of dimension 24cm², weight 65g, and was placed in the lumbar lordosis
207 curve, between the second and the third lumbar vertebrae, close to the subject's center of mass.
208 Each detector includes a 3-axis linear accelerometer coupled to two 3-axis gyroscopes. The device
209 is controlled with a tablet connected via Bluetooth and collects a one-lead ECG at 200Hz
210 (ADS1292R, ADInstruments) and the BCG and SCG signals at 50Hz, as previously described (18,
211 33, 34) .

212

213 1.3 Data analysis

214 1.3.1 MSNA analysis

215 The identification of the apnea was based on the respiratory signal measured with the
216 respiratory belt: the beginning of the apnea was identified at the end of a maximal expiration, the
217 lungs being at their residual volume, the end of the apnea was identified prior to the restauration
218 of respiration. The duration of the apnea differed between individuals; each of them was required
219 to hold his breath as long as he could (from a minimum of 13 seconds to a maximum of 49
220 seconds). The period of normal respiration prior to the apnea is referred to as "baseline" and lasts
221 on average 50s. The apneic episode was split up in three equal epochs, defined as "1/3 apnea",
222 "2/3 apnea", "3/3 apnea" and subsequently analyzed. In our previous work (34) we
223 quantitatively analyzed the evolution of *iK* continuously beat-by-beat during a 10s length end-
224 expiratory apnea, and found that the *iK* dropped at the beginning of the apnea compared to
225 normal breathing, and increased progressively towards the end of the apnea to values comparable
226 to those of normal breathing. While cardiac energies can be calculated for each contractile cycle,
227 MSNA does not appear for every heartbeat (48) so that a beat-by-beat analysis was not applicable
228 in the present investigation. Thus, to quantitatively evaluate simultaneous changes of *iK* and

229 MSNA along the course of apnea authors decided to split the apneic episode in three equal parts,
230 in order to analyze the evolution of iK and MSNA all over the apnea. This approach of splitting an
231 apneic episode in more than one component is not new: Shimizu et al. divided the apnea in two
232 parts to compare the sympathetic activity at the beginning and at the end of the apnea (48); Somers
233 VK. et al. had already divided a 20s length apnea in four equal parts of 5 seconds each to analyse
234 MSNA and BP changes all along the apneic episode (50). Also, with regards to obstructive sleep
235 apnea, it is well known that the sympathetic tone does change profoundly at the end of the apnea
236 compared to the beginning (49) underlying further the concept that the sympathetic activity, as
237 well as other cardiovascular events, profoundly evolve along the course of an apneic episode.

238 The MSNA signal identification consisted in the visual inspection of the neurogram by a
239 trained operator. First, a low pass digital filter was applied to automatically filter the unwanted
240 noise in the signal. Second, the baseline was normalized to reduce the signal to noise ratio, as
241 previously described (67). Third, the start and the end of each burst were manually identified and
242 all the bursts numbered successively. For this purpose, each burst needed to disclose at least a 3:1
243 signal to noise ratio (67). Then, the amplitude of each burst was automatically computed with the
244 specific module "Peak Analysis" of LabChart version 8.0 (ADInstrument).

245 The sympathetic activity was expressed as burst frequency (BF), defined as the number of
246 burst per minute, and as total MSNA activity (tMSNA), computed as burst per minute multiplied
247 by mean burst amplitude, as previously described (60, 63).

248 Since the apnea duration was highly different between subjects and all less than one minute,
249 the number of bursts identified during each epoch of the apnea was normalized for the duration of
250 each epoch itself.

251

252 1.3.2 BCG and SCG signaling processing

253 The BCG and SCG records were temporally synchronized with the other physiological
254 parameters described above. A specific Toolbox written in Matlab (Mathwork® version 2019b)

255 allowed the visual inspection of the BCG and SCG waveforms, the identification of the apnea and
 256 the computation of the iK metrics. With this tool, the operator could examine the quality of the
 257 record and select a temporal window of individual consecutive beats. The beats sampled in the
 258 selected temporal region were identified based on the automatic detection of the peak ECG-R
 259 wave. Ensemble Averaging (EA) on all beats over the selected time period was performed and
 260 scalar parameters of iK_{Lin} and iK_{Rot} were automatically computed (figure 1). This method of
 261 sampling and averaging allows to generate an averaged BCG/SCG signal which best fits the shape
 262 of a cardiac cycle. Additionally, the EA allows to partially remove motion artifacts of the signals.
 263 P, Q, R, S, T waves on the ECG were automatically identified and used as reference points for the
 264 identification of the electrical cardiac cycle. The sum of PQ, QRS, ST and TP' defined a whole
 265 cardiac cycle (CC).

266 The iK was calculated for both the BCG and SCG signals during the baseline and during
 267 the first, the second and the last third of the apnea. From the integration with respect to time of
 268 linear accelerations of the BCG and SCG signals, linear velocities can be obtained, and the linear
 269 kinetic energy can be computed as follow:

$$270 \quad K_{Lin} = \frac{1}{2} m (v_x^2 + v_y^2 + v_z^2) \quad (1)$$

271 where m is the mass of the subject, K_{Lin} is the linear kinetic energy, v_x^2, v_y^2, v_z^2 are components of the
 272 linear velocity vector \vec{v} obtained by integrating the accelerations acquired by the accelerometers at
 273 both BCG and SCG positions with respect to time. The integration of equation (1) computed for a
 274 cardiac cycle (CC) gives the content of energy in the linear dimension (iK_{Lin}) for that cardiac cycle:

$$275 \quad iK_{Lin} = \int_{CC} K_{Lin} \cdot dt \quad (2)$$

276 From angular velocities recorded with the BCG and SCG, the rotational kinetic energy can be
 277 computed as follow:

$$278 \quad K_{Rot} = \frac{1}{2} (I_{xx} \omega_x^2 + I_{yy} \omega_y^2 + I_{zz} \omega_z^2) \quad (3)$$

279 where K_{Rot} is the rotational kinetic energy, I_{xx} , I_{yy} , I_{zz} are the orthogonal components of the
280 moment of inertia, $\vec{\omega}$ is the angular velocity (with its components ω_x^2 , ω_y^2 , ω_z^2). The integration of
281 equation (3) computed for a cardiac cycle gives the content of energy in the rotational dimension,
282 iK_{Rot} , of a cardiac cycle:

$$283 \quad iK_{Rot} = \int_{CC} K_{Rot} \cdot dt \quad (4)$$

284 More details about this method can be found in (18, 31, 33, 34).

285 Several factors can contaminate the BCG and SCG signals, as respiration, involuntary
286 movements, cough... To reduce contamination signals from artifacts, an automatic outlier
287 detection was applied on beats that would generate too large energies. If the iK of a heartbeat was
288 higher than 5 times the median of the respective kinetic energy of the 5 previous beats, the iK of
289 the concerned heartbeat was considered compromised by an external artefact and classified as
290 abnormal. This was done within a specific state, e.g baseline or apnea.

291 Respiration might influence the BCG and SCG signals in three different ways: by producing a
292 wandering of the baseline as a result of chest movement, by modifying the amplitude of SCG due
293 to intra-thoracic pressure variation and through the induced RR interval changes during the
294 respiratory cycle. To avoid contamination signal from respiratory movement, a high-pass filter
295 was applied to the signals.

296

297 *1.4 Statistical analysis*

298 The symmetry of distributions was assessed by the Kolmogorov-Smirnov test and Shapiro-Wilk
299 test. The Wilcoxon sign-rank test was used to evaluate differences in variables between normal
300 respiration and the apnea. Variables were presented as medians and interquartile range [IR] or
301 means and standard deviations (\pm SD). ANOVA or Kruskal Wallis tests were applied according to
302 data distribution to assess the evolution of variables throughout the three different phases of the
303 apnea. Bonferroni correction was applied to account for multiples comparisons.

304 Associations of changes of cardiac kinetic energies with changes of MSNA activity were assessed
 305 using the Spearman's or Pearson's correlation, according to data distribution.

306 Analyses were performed using SPSS® 22.0 on Windows.

307

308 **RESULTS**

309 Baseline characteristics and modifications of hemodynamic (HR, BP) and respiratory (SatO₂,
 310 ETCO₂) parameters during the apnea along with MSNA activity (BF, tMSNA) are reported in table

311 1.

312

Table 1. Modifications of hemodynamic parameters along with metrics of MSNA activity during the baseline and the apnea.			
Parameter	Baseline	Apnea	p-value
SBP (mmHg)	115 ± 11	120 ± 12	0.01
DBP (mmHg)	59 ± 9	61 ± 11	0.1
MBP (mmHg)	79 ± 10	82 ± 13	0.1
HR (bpm)	65 ± 7	67 ± 11	0.2
SatO₂ (%)	97 ± 2	96 ± 4	0.02
ETCO₂ (mmHg)	40 ± 3	42 ± 5	0.1
BF (burst/min)	18.9 ± 9.9	28.4 ± 10.6	0.002
tMSNA (AU/min)	46.7 [28.8; 63.8]	84.0 [59.9; 184.5]	0.001
SBP, systolic blood pressure (mmHg); DBP, diastolic blood pressure (mmHg); MBP, mean blood pressure (mmHg); PP, pulse pressure (mmHg); HR, heart rate (bpm); SatO ₂ , oxygen saturation (%); ETCO ₂ , end-tidal CO (mmHg); BF, burst frequency (burst/min); tMSNA, total MSNA activity (AU/min). Data are presented as mean ± SD			

or median [P25; P75] according to data distribution.

313

314 Oxygen saturation decreases during the apnea compared to baseline ($p=0.02$). SBP increases
315 during the apnea compared to baseline ($p=0.01$). MSNA activity rises from baseline to apnea as
316 well ($p=0.002$; $p=0.001$ for BF and tMSNA, respectively).

317 In table 2, the apnea has been divided in three equal epochs (1/3 apnea, 2/3 apnea, 3/3 apnea) and
318 results are presented according to the phase.

Table 2. Modifications of metrics of MSNA activity, iK of SCG and BCG from baseline to the end of the apnea.					
Parameters	Baseline	1/3 apnea	2/3 apnea	3/3 apnea	p_{ALL}
BF (burst/min)	18.9 ± 9.9	23.9 ± 21.7	26.2 ± 16.2	37.3 ± 18.0	0.02
tMSNA (AU/min)	46.7 [28.8; 63,8]	57.8 [10.6; 137.9]	76.5 [30.5; 182.3]	128.7 [70.3; 308.5]	0.01
iK_{Lin}^{SCG} (μJ.s)	100 [80; 100]	100 [60; 180]	110[70; 190]	110[80; 190]	0.46
iK_{Rot}^{SCG} (nJ.s)	0.9 [0.5; 1.3]	0.9 [0.5; 1.3]	1.1 [0.6; 1.8]	1.1 [0.4; 1.9]	0.12
iK_{Lin}^{BCG} (μJ.s)	7.6 [5.5; 12.5]	8.8 [7.0; 1400]	200 [6.7; 1600]	9.3 [6.5; 1500]	0.03
iK_{Rot}^{BCG} (μJ.s)	2.9 [1.5; 4.5]	3.6 [3.0; 4.7]	3.4 [2.9; 5.3]	3.3 [2.9; 5.2]	0.0005
BF, burst frequency (burst/min); tMSNA, total MSNA activity (AU/min); iK_{Lin}^{SCG} (μJ.s) and iK_{Rot}^{SCG} (nJ.s), integral of kinetic energy of the SCG in the linear and rotational dimension, respectively; iK_{Lin}^{BCG} (μJ.s) and iK_{Rot}^{BCG} (μJ.s) integral of kinetic energy of the BCG in the linear and rotational dimension, respectively;					

Data are presented as mean \pm SD or median and [P25; P75] according to data distribution.

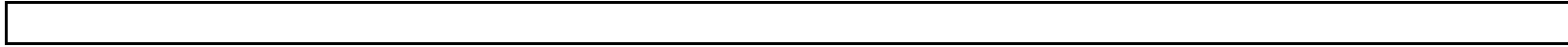
320

321 Sympathetic activity changes progressively throughout the apnea, with a rise of the BF and
322 tMSNA from baseline to the end of the apnea ($p=0.02$, $p=0.01$, respectively, table 2). According to
323 multiple comparison analysis, BF increased by 97% from baseline to the last third of apnea,
324 ($p=0.003$). tMSNA increased by 64% and 176% from baseline to the second and to last third of the
325 apnea ($p=0.04$, $p=0.005$, respectively).

326 With regards to the SCG, the iK did not change during the apnea, neither in the linear nor in the
327 rotational dimension. With regards to the BCG, the iK changed significantly in both dimensions
328 ($p=0.03$, $p=0.0005$ for the linear and rotational dimension, respectively). In particular, when
329 considering multiple comparisons, iK_{Lin}^{BCG} increased by 58% from baseline to the second third of the
330 apnea ($p=0.02$). In the rotational dimension, iK_{Rot}^{BCG} increased by 20% from baseline to the first third
331 of the apnea ($p=0.02$). Figure 2 displays a representative example of modifications of MSNA along
332 with kinetic energy of BCG during a maximal end-expiratory apnea.

333 In table 3, correlations between changes of MSNA parameters and changes of iK during the apnea,
334 both expressed in %, are reported. Particularly, the differences between: BSL and 1/3 apnea; BSL
335 and 2/3 apnea; BSL and 3/3 apnea have been normalized for the baseline for each variable and
336 expressed in %.

Table 3. Correlation analysis of ΔiK of BCG and SCG with ΔBF and $\Delta tMSNA$ for each epoch of apnea.				
<i>N</i> = 16	ΔiK_{Lin} BCG	ΔiK_{Rot} BCG	ΔiK_{Lin} SCG	ΔiK_{Rot} SCG
<i>BSL and 1/3 apnea</i>				
$\Delta tMSNA$	$r = 0.13, p = 0.65$	$r = 0.009, p = 0.94$	$r = -0.02, p = 0.95$	$r = -0.06, p = 0.83$
ΔBF	$r = -0.003, p = 0.97$	$r = 0.01, p = 0.97$	$r = -0.13, p = 0.65$	$r = 0.008, p = 0.98$
<i>BSL and 2/3 apnea</i>				
$\Delta tMSNA$	$r = 0.45, p = 0.055$	$r = 0.09, p = 0.73$	$r = 0.44, p = 0.09^*$	$r = -0.25, p = 0.34^*$
ΔBF	$r = 0.52, p = 0.04$	$r = 0.18, p = 0.52$	$r = 0.51, p = 0.04^*$	$r = -0.22, p = 0.41^*$
<i>BSL and 3/3 apnea</i>				
$\Delta tMSNA$	$r = 0.85, p < 0.0001$	$r = -0.17, p = 0.95$	$r = 0.62, p = 0.01$	$r = 0.06, p = 0.08$
ΔBF	$r = 0.72, p = 0.002$	$r = -0.03, p = 0.93$	$r = 0.49, p = 0.06$	$r = 0.14, p = 0.62$
<p>Pearson's correlation of ΔiK (%) of BCG and SCG with $\Delta tMSNA$ and ΔBF (%). The differences (Δ) between: BSL and the 1/3 of apnea; BSL and the 2/3 of apnea; BSL and the 3/3 of apnea have been normalized for the BSL and are expressed in %.</p> <p>BCG, ballistocardiography; SCG, seismocardiography; BF, burst frequency; iK_{Lin} and iK_{Rot}, linear and rotational kinetic energies, respectively; tMSNA, total muscular sympathetic nerve activity. * Spearman correlation.</p>				



339 When considering the difference of tMSNA and BF between BSL and the first third of apnea, no
340 correlations were found with the corresponding difference of iK . When the difference between BSL
341 and the second third of apnea is considered for each variable, ΔiK_{Lin} of BCG and SCG are mildly
342 related to the ΔBF ($0.51 < r < 0.52$, both $p=0.04$). When the difference between BSL and the last third
343 of apnea is considered for each variable, strong correlations were found between ΔiK_{Lin} of BCG
344 and $\Delta tMSNA$ and ΔBF ($r = 0.85$, $p < 0.0001$; $r = 0.72$, $p = 0.002$, respectively) and between ΔiK_{Lin} of
345 SCG and $\Delta tMSNA$ ($r = 0.62$, $p = 0.01$).

346 Results of correlations between iK metrics and MSNA parameters for the last third of the apnea are
347 reported in figure 3. In this figure, the point with the highest tMSNA value is not an outlier and
348 corresponds to a subject which presented a striking rise in MSNA during the apnea (figure 2).

351 **DISCUSSION**

352

353 We report for the first time the direct evidence of a positive relation between changes of
354 cardiac kinetic energy, computed from BCG and SCG signals, and changes of sympathetic activity
355 assessed by direct intra neural recordings of sympathetic nerve traffic, during a maximal voluntary
356 end-expiratory apnea, especially at the end of the apnea compared to normal breathing. Indeed,
357 while at the beginning of the apnea changes of sympathetic activity, expressed in %, were not
358 related to any of the changes of *iK* parameters, expressed in % as well, at the end of the apnea
359 changes of sympathetic activity were strongly related to changes of *iK* parameters, particularly the
360 *iK* of BCG in the linear dimension. These results lead authors to believe that there is a link between
361 the increased sympathetic activity and the cardiac kinetic energy, in particular when activation of
362 SNS is stronger, as it is the case at the end of a sustained apnea. Additionally, the linear cardiac
363 kinetic energy, rather than the rotational one, computed from the BCG seems to better correlate
364 with sympathetic activity. Based on this finding, authors speculate that the linear kinetic energy,
365 rather than the rotational one, may provide information on the myocardial contractility status in
366 this restricted context of SNS overactivity.

367 We have previously highlighted the potential of BCG and SCG in providing reliable
368 information on cardiac function (18, 35): metrics of *iK* can follow changes in cardiac contractility
369 under dobutamine stimulation and are related to SV and CO (18).

370 Because of the close connection between the respiratory and cardiovascular systems,
371 metrics of *iK* secured from BCG and SCG waveforms profoundly change in relation to specific
372 respiratory events (33, 34). As previously demonstrated (34), the kinetic energy produced by
373 cardiac contraction during inspiration is higher than the one during expiration and, during a 10
374 seconds length end-expiratory apnea, is higher compared to normal breathing and it increases
375 progressively from the beginning to the end of the apnea.

376 Results from the present investigation confirm those of the previous ones and add the novelty that
377 the modifications of the cardiac kinetic energy observed during the apnea may be related to the
378 MSNA activity.

379 The diving reflex, or response, is a set of physiological adaptations in response to
380 immersion and triggered by breath holding (13, 28), which primary role is to relocate oxygenated
381 blood to hypoxic sensitive tissues, heart and brain first (1, 12). The physiological patterns involved
382 in the diving response are bradycardia, increased secretion of adrenal catecholamines and
383 peripheral and visceral capillary bed vasoconstriction, the latter is the primary event occurring
384 during the diving response (11) as a result of increased sympathetic outflow to the periphery (12).
385 Even if the diving response can be triggered solely by respiratory arrest (12, 24), hypoxia (24, 27,
386 29, 46, 63, 69) and hypercapnia (24, 39, 55, 69) are additional potent stimuli to further booster the
387 sympathetic outflow. Consequences of sympathetic overactivity during the diving response are
388 increased vascular resistance (17, 27), increased blood pressure (17, 27) and reflex bradycardia (1,
389 56). However, in the present investigation we, as other predecessors (4, 10, 17, 40, 60) did not
390 observe any bradycardia.

391 Breath holding profoundly changes not only peripheral vascular function but influence also
392 cardiac functions and morphology (5, 10, 43). During prolonged end-expiratory apnea, increased
393 left ventricular end-diastolic and end-systolic volume (LVEDV, LVESV, respectively) (5, 10, 43),
394 along with a rise of SV (10, 43) and CO (5, 43) and relocation of blood flow into the ascending aorta
395 (10), occur.

396 Acknowledged that the *iK* of BCG and SCG is an indirect measure of SV and CO (18) the
397 increased *iK*, observed mainly during the end of the apnea, may reflect the positive cardiac
398 inotropism and the increased of SV, CO along with the relocation of blood flow into the ascending
399 aorta, even if not directly measured, as a consequence of increased sympathetic outputs and
400 cardiovascular adaptations occurring during the diving response. The association between
401 changes of *iK* and changes of MSNA parameters is more evident at the end of the apnea compared

402 to normal breathing and sympathetic activity seems to be stronger related to the kinetic energy of
403 BCG rather than the one of SCG, likely due to the better estimation of SV and CO with the BCG
404 than with the SCG, as previously demonstrated (18). Indeed, the BCG signal is generated by the
405 recoil forces generated by cardiac contraction and blood flow ejection acting on the vasculature of
406 the main vessels at each heartbeat (54). Since the SV is the amount of blood ejected into the
407 vasculature at each cardiac contraction, and the CO is the SV per unit of time, the metrics secured
408 from BCG are better related to SV and CO than the SCG as previously reported (18). Another
409 possible explanation of this discrepancy between the BCG and SCG is that, since the resultant SCG
410 signal is generated by several physiologic phenomena including not only cardiac contraction, but
411 also heart valves closure and opening, blood turbulence, momentum changes (57), the sum of
412 these phenomena other than cardiac contraction only, may be responsible for the weaker
413 correlation with the MSNA activity observed.

414 A number of home sleep apnea testing (HAST) are nowadays available to meet the
415 increasing demand of sleep apnea disordered monitoring (26, 42). HAST have been developed for
416 years and they include a large spectrum of devices, as oxygen saturation, heart rate, oral/nasal
417 outflow, respiratory effort, body position detectors (32) and also contactless technologies for
418 detection of respiration, body movements, heart beats (38, 42). Cardiovascular parameters as blood
419 pressure and stroke volume can be monitored during sleep continuously through finger
420 photoplethysmography, but the pressure applied to the finger is not comfortable for the patients,
421 thus hampering the compliance to the device (42). The novelty of the modern BCG and SCG
422 described in this paper is that they can quantitatively estimate the « strength » or « weakness » of
423 the cardiac muscle, expressed in term of kinetic energy, during an apneic episode, thus adding
424 complementary values to the already existing technology for sleep disturbances
425 diagnosis/monitoring. This technology is non intrusive, can be remotely controlled and measures
426 of *iK* can be computed automatically. With this information before us, modern BCG and SCG
427 should be seen not as competitors to the already exiting devices for home sleep monitoring, but

428 complementary to them, for this technology has the potential to provide new insights on the
429 cardiovascular system.

430 Our new observation that there is a link between BCG/SCG metrics and intraneural
431 changes in sympathetic activity during apneas suggests that this technology may prove useful for
432 the diagnosis or the follow-up of respiratory-related sleep disturbances in further studies.

433 However, before this can be tested, there are still important technical challenges ahead. To name a
434 few, the artefacts generated by body movements on the BCG and SCG signals may prove
435 challenging. Displacement of the BCG and SCG recorders during sleep is another possible pitfall.
436 Last, the management of the sustained data flow generated by an overnight BCG and SCG
437 recording might represent another hurdle.

438

439 *Limitations*

440 The sample size was small and counted only 28 volunteers of which 10 had to be ruled out
441 because of technical difficulties in locating the peroneal nerve during the experimental procedure.
442 The microneurography is a demanding technique, where the active needle inserted in the
443 implanted nerve is freely floating into the subdermal tissues, making an eventual stabilization
444 impossible (59, 67). The loss of the neurogram after nerve identification was thus frequent,
445 explaining the high rate of lost neurograms (35%). The small sample size may hamper the
446 correlation analysis between *iK* and MSNA parameters and the subsequent interpretation of
447 results.

448

449 Another limitation to note is the interpretation of the neurogram, which is a subjective
450 procedure. To choose the apnea to be analyzed and to make the interpretation of the neurogram
451 less subjective, we closely followed the standards described in (67): a steady baseline without
452 fluctuations; bursts clearly visible above the baseline noise; a steady baseline noise amplitude all
453 over the selected region.

454

455 Another important limitation to consider is the duration of the apnea and the subsequent
456 MSNA analysis and interpretation. Indeed, as explained in (37), the reliability of MSNA depends
457 on the durations of the selected time window and loss of reliability is observed for epochs below
458 15 seconds length. In the present investigation, while the baseline mean duration is of 50 seconds,
459 the apnea duration widely varies, for it was submitted to the subject capability of breath holding.
460 Imposing a 45 seconds length apnea, in order to have three equal epochs of 15s length, to non-
461 trained volunteers was not feasible and probably not ethically correct. For these reasons we asked
462 the participant to perform a sustained end-expiratory apnea at the best of his capacities.
463 Additionally, even if for epochs below 15s MSNA may lose validity and reliability, it should be
464 noted that in the real clinical setting, the duration of an apneic episode varies much in the same
465 subject with important cardiovascular consequences (2, 68). This means that in the real clinical
466 setting, apneic episodes as short as 15s or shorter should be considered as they may have
467 cardiovascular consequences. Additionally, MSNA analysis have already been performed on
468 apnea episodes shorter than 15 seconds (49, 50).

469

470 Analysis of spectral components of MSNA has not been performed in the present
471 investigation. Indeed, to perform a spectral analysis, long and steady state periods are required,
472 which was not the case in this study, as each part of the apnea lasted few seconds.
473 Additionally, during the apnea, the high frequency (HF) component is lost at some extent,
474 making the LF/HF analysis more trivial to analyze (60). The relationship between kinetic energy
475 and spectral components of MSNA is a topic of great interest and should be the object of
476 another study under different experimental conditions.

477

478 We did not measure directly arterial gases pressures, pO_2 and pCO_2 , so we could not
479 directly evoke hypoxia and/or hypercapnia as trigger factors for sympathetic tone activation.
480 However, $SatO_2$ is widely used as surrogate for arterial oxygen saturation (3, 25) and it reliably
481 estimates arterial saturation for values above 75% (7).

482

483 We did not perform echocardiography to measure cardiac parameters as well as cardiac
484 chambers volume, SV, and CO. These parameters have been indirectly invoked to explain changes
485 in iK based on previous findings (18). In mitigation however, to achieve an acceptable
486 echocardiographic window, the subjects would have been asked to move from a dorsal
487 recumbence to a semi lateral supine position. Such a displacement has a very high likelihood to
488 displace the microneurographic electrode. Last, the pressure of the echocardiographic probe on the
489 thoracic wall would have jeopardized the BCG and SCG signals. These technical limitations
490 explain that echocardiographic parameters were not foreseen in the study design.

491

492 The present investigation is a pilot study including exclusively healthy man to test the
493 hypothesis on whether increased cardiac kinetic energy as computed from the BCG and SCG
494 signals might be linked to sympathetic tone activation during an end-expiratory apnea. Further
495 studies are needed to confirm the causal-effect relationship between variations of cardiac kinetic
496 energy and the autonomic nervous system in different setups. For example, it should be
497 investigated the relationship between sympathetic activity and cardiac kinetic energies in a context
498 of chronic heart failure, where the autonomic system is profoundly impaired with a shift to
499 sympathetic over activity (30, 61); disruption of the autonomic balance is observed also in
500 obstructive sleep apnea syndrome, with an increased sympathetic activity (49) and it would be
501 interesting to analyze the relationship between cardiac kinetic energies and sympathetic activity in
502 these conditions.

503

504 **Conclusions**

505 During a maximal voluntary end-expiratory apnea, the *iK* computed from the BCG and SCG
506 signals increased compared to normal respiration. The novelty of the present investigation is that
507 the increased cardiac kinetic energy is linked to the overactivity of sympathetic nervous system,
508 especially at the end of a sustained end-expiratory apnea, likely reflecting the rise of SV and CO
509 and the positive cardiac inotropism secondary to the increased sympathetic outputs occurring
510 during the diving response.

511

512 **PERSPECTIVES AND SIGNIFICANCE**

513 Modern multi-dimensional ballistocardiography and seismocardiography can provide new
514 insights to the cardiovascular system through the window of micro-accelerations, by computing
515 the kinetic energy produced by the cardiac muscle during a contractile cycle. This renewed
516 technology may complement the existing ones for the evaluation of cardiovascular system, by
517 providing information on the contractility status of the cardiac muscle beat-by-beat. In this light,
518 while it is well acknowledged that during an apneic episode the sympathetic activity rises with a
519 shift of the autonomic balance towards the sympathetic arm, less is now about changes of cardiac
520 contractility during the apnea. This technology revealed that along with the surge of sympathetic
521 activity, also the cardiac kinetic energy rises during prolonged breath holding and that this surge
522 is linked to the sympathetic overactivity. These findings may be extended to several
523 cardiovascular diseases characterized by an imbalance of the autonomic system, as chronic heart
524 failure and obstructive sleep apnea, in order to study the relationship between cardiac kinetic
525 energies and sympathetic activity in these conditions.

526

527 **Authors contributions**

528 A.G. J-B.P.W. and P.V.D.B. conceived the idea and the design of the study. S.M. and A.G.
529 carried out the whole experimental procedure, from the recruitment of volunteers to
530 conducting the experimental session. S.M. had full access to all data in the present investigation

531 and takes responsibility for the integrity of the data and the accuracy of the data analysis. Ju.R.
532 performed statistical analysis. A.H. provided the technical support for the correct extrapolation
533 of all the metrics from SCG and BCG. S.M. drafted the manuscript. A.G., A.H., J.R., D.G.,
534 P.F.M., and P.V.D.B. revised the manuscript critically for important intellectual content. All the
535 authors proofread and made corrections to this manuscript.
536

537 **Acknowledgements**

538 The authors would like to acknowledge the contribution of the volunteers and staff members of
539 the Cardiology Department of the Erasme-Hospital. Authors thank the “Fonds Erasme”
540 foundation and the “Fonds National pour la Recherche Scientifique (FNRS)” for the financial
541 support of the present investigation.
542

543 **Sources of Fundings**

544 This work was supported by the “Fonds Erasme pour le Recherche Médicale” (S.M.); by “le fond
545 Biowin, The health cluster of Wallonia” (A.G. J-B.P.W.); by the “FNRS, Fonds National pour la
546 Recherche Scientifique”, Fédération Wallonie Bruxelles, Belgium (S.M., J.R.), by a grant from the
547 European Space Agency and the Belgian Federal Scientific Policy Office (PRODEX PEA
548 4000110826) (A.H., P.F.M).
549

550 **Conflict of interests**

551 P-F. Migeotte, D. Gorlier and A. Hossein declare having direct ownership of shares in Healthcare
552 Company.

553 REFERENCES

- 554 1. **Alboni P, Alboni M, and Gianfranchi L.** Diving bradycardia: a mechanism of defence against
555 hypoxic damage. *J Cardiovasc Med (Hagerstown)* 12: 422-427, 2011.
- 556 2. **Alex R, Manchikata S, Machiraju K, Altuwaijri E, Watenpaugh DE, Zhang R, and**
557 **Behbehani K.** Effect of apnea duration on apnea induced variations in cerebral blood flow velocity
558 and arterial blood pressure. *Conf Proc IEEE Eng Med Biol Soc* 2014: 270-273, 2014.
- 559 3. **Ascha M, Bhattacharyya A, Ramos JA, and Tonelli AR.** Pulse Oximetry and Arterial Oxygen
560 Saturation during Cardiopulmonary Exercise Testing. *Med Sci Sports Exerc* 50: 1992-1997, 2018.
- 561 4. **Badra LJ, Cooke WH, Hoag JB, Crossman AA, Kuusela TA, Tahvanainen KU, and Eckberg**
562 **DL.** Respiratory modulation of human autonomic rhythms. *Am J Physiol Heart Circ Physiol* 280:
563 H2674-2688, 2001.
- 564 5. **Batinic T, Utz W, Breskovic T, Jordan J, Schulz-Menger J, Jankovic S, Dujic Z, and Tank J.**
565 Cardiac magnetic resonance imaging during pulmonary hyperinflation in apnea divers. *Med Sci*
566 *Sports Exerc* 43: 2095-2101, 2011.
- 567 6. **Calvo M BJ, Le Rolle V, Lemonnier M, Yasuda S, Oosterlinck W, Hernandez A.** . Evaluation
568 of Three-Dimensional Accelerometers for the Study of Left Ventricular Contractility. In: *Computing*
569 *in Cardiology Conference (CinC)*. Maastricht, Netherlands: IEEE, 2018.
- 570 7. **Chapman KR, Liu FL, Watson RM, and Rebeck AS.** Range of accuracy of two wavelength
571 oximetry. *Chest* 89: 540-542, 1986.
- 572 8. **De Lalla V, Jr., and Brown HR, Jr.** Respiratory variation of the ballistocardiogram. *Am J Med*
573 9: 728-733, 1950.
- 574 9. **Desruelles J MJ, Debacker G.** Seminar on Ballistocardiography. Practical Value of the
575 Ballistocardiogram in Myocardial Infarction. *Am J Cardiol* 3: 236-241, 1959.
- 576 10. **Eichhorn L, Doerner J, Luetkens JA, Lunkenheimer JM, Dolscheid-Pommerich RC,**
577 **Erdfelder F, Fimmers R, Nadal J, Stoffel-Wagner B, Schild HH, Hoeft A, Zur B, and Naehle CP.**
578 Cardiovascular magnetic resonance assessment of acute cardiovascular effects of voluntary
579 apnoea in elite divers. *J Cardiovasc Magn Reson* 20: 40, 2018.
- 580 11. **Fagius J, and Sundlof G.** The diving response in man: effects on sympathetic activity in
581 muscle and skin nerve fascicles. *J Physiol* 377: 429-443, 1986.
- 582 12. **Foster GE, and Sheel AW.** The human diving response, its function, and its control. *Scand J*
583 *Med Sci Sports* 15: 3-12, 2005.
- 584 13. **Gooden BA.** Mechanism of the human diving response. *Integr Physiol Behav Sci* 29: 6-16,
585 1994.
- 586 14. **Gordan R, Gwathmey JK, and Xie LH.** Autonomic and endocrine control of cardiovascular
587 function. *World J Cardiol* 7: 204-214, 2015.
- 588 15. **Guelen I, Westerhof BE, Van Der Sar GL, Van Montfrans GA, Kiemeneij F, Wesseling KH,**
589 **and Bos WJ.** Finometer, finger pressure measurements with the possibility to reconstruct brachial
590 pressure. *Blood Press Monit* 8: 27-30, 2003.
- 591 16. **Gurev V, Tavakolian K, Constantino J, Kaminska B, Blaber AP, and Trayanova NA.**
592 Mechanisms Underlying Isovolumic Contraction and Ejection Peaks in Seismocardiogram
593 Morphology. *J Med Biol Eng* 32: 103-110, 2012.
- 594 17. **Heusser K, Dzamonja G, Tank J, Palada I, Valic Z, Bakovic D, Obad A, Ivancev V, Breskovic**
595 **T, Diedrich A, Joyner MJ, Luft FC, Jordan J, and Dujic Z.** Cardiovascular regulation during apnea in
596 elite divers. *Hypertension* 53: 719-724, 2009.
- 597 18. **Hossein A, Mirica DC, Rabineau J, Rio JID, Morra S, Gorlier D, Nonclercq A, Borne PV, and**
598 **Migeotte PF.** Accurate Detection of Dobutamine-induced Haemodynamic Changes by Kino-

- 599 Cardiography: A Randomised Double-Blind Placebo-Controlled Validation Study. *Sci Rep* 9: 10479,
600 2019.
- 601 19. **Inan OT, Baran Pouyan M, Javaid AQ, Dowling S, Etemadi M, Dorier A, Heller JA, Bicen**
602 **AO, Roy S, De Marco T, and Klein L.** Novel Wearable Seismocardiography and Machine Learning
603 Algorithms Can Assess Clinical Status of Heart Failure Patients. *Circ Heart Fail* 11: e004313, 2018.
- 604 20. **Inan OT, Migeotte PF, Park KS, Etemadi M, Tavakolian K, Casanella R, Zanetti J, Tank J,**
605 **Funtova I, Prisk GK, and Di Rienzo M.** Ballistocardiography and seismocardiography: a review of
606 recent advances. *IEEE J Biomed Health Inform* 19: 1414-1427, 2015.
- 607 21. **Izzo JL, Jr., and Taylor AA.** The sympathetic nervous system and baroreflexes in
608 hypertension and hypotension. *Curr Hypertens Rep* 1: 254-263, 1999.
- 609 22. **Jafari Tadi M, Lehtonen E, Saraste A, Tuominen J, Koskinen J, Teras M, Airaksinen J,**
610 **Pankaala M, and Koivisto T.** Gyrocardiography: A New Non-invasive Monitoring Method for the
611 Assessment of Cardiac Mechanics and the Estimation of Hemodynamic Variables. *Sci Rep* 7: 6823,
612 2017.
- 613 23. **Johnson CD, Roe S, and Tansey EA.** Investigating autonomic control of the cardiovascular
614 system: a battery of simple tests. *Adv Physiol Educ* 37: 401-404, 2013.
- 615 24. **Jouett NP, Watenpaugh DE, Dunlap ME, and Smith ML.** Interactive effects of hypoxia,
616 hypercapnia and lung volume on sympathetic nerve activity in humans. *Exp Physiol* 100: 1018-
617 1029, 2015.
- 618 25. **Kackmarek RK SJ, Heuer AJ.** . Analysis and Monitoring of GAs Exchange. In: *Egan's*
619 *Fundamental of Respiratory Care*, edited by Mosby 2012, p. 398.
- 620 26. **Kapur VK, Auckley DH, Chowdhuri S, Kuhlmann DC, Mehra R, Ramar K, and Harrod CG.**
621 Clinical Practice Guideline for Diagnostic Testing for Adult Obstructive Sleep Apnea: An American
622 Academy of Sleep Medicine Clinical Practice Guideline. *J Clin Sleep Med* 13: 479-504, 2017.
- 623 27. **Leuenberger UA, Hardy JC, Herr MD, Gray KS, and Sinoway LI.** Hypoxia augments apnea-
624 induced peripheral vasoconstriction in humans. *J Appl Physiol (1985)* 90: 1516-1522, 2001.
- 625 28. **Lindholm P, and Lundgren CE.** The physiology and pathophysiology of human breath-hold
626 diving. *J Appl Physiol (1985)* 106: 284-292, 2009.
- 627 29. **Lusina SJ, Kennedy PM, Inglis JT, McKenzie DC, Ayas NT, and Sheel AW.** Long-term
628 intermittent hypoxia increases sympathetic activity and chemosensitivity during acute hypoxia in
629 humans. *J Physiol* 575: 961-970, 2006.
- 630 30. **Mark AL.** Sympathetic dysregulation in heart failure: mechanisms and therapy. *Clin Cardiol*
631 18: 13-8, 1995.
- 632 31. **Migeotte PF, Mucci V., Delière Q., Lejeune L., van de Borne P.** Multi-dimensional
633 Kinetocardiography a New Approach for Wearable Cardiac Monitoring Through Body Acceleration
634 Recordings. *XIV Mediterranean Conference on Medical and Biological Engineering and Computing*
635 1125-1130, 2016.
- 636 32. **Miller JN, Schulz P, Pozehl B, Fiedler D, Fial A, and Berger AM.** Methodological strategies
637 in using home sleep apnea testing in research and practice. *Sleep Breath* 22: 569-577, 2018.
- 638 33. **Morra S, Hossein A, Gorlier D, Rabineau J, Chaumont M, Migeotte PF, and van de Borne**
639 **P.** Ballistocardiography and Seismocardiography detect hemodynamic changes during simulated
640 obstructive apnea. *Physiol Meas* 2020.
- 641 34. **Morra S, Hossein A, Gorlier D, Rabineau J, Chaumont M, Migeotte PF, and van de Borne**
642 **P.** Modification of the mechanical cardiac performance during end-expiratory voluntary apnea
643 recorded with ballistocardiography and seismocardiography. *Physiol Meas* 40: 105005, 2019.
- 644 35. **Morra S. and Hossein A. RJ, Gorlier D., Racape J., Migeotte PF., van de Borne P.** Left
645 ventricle mechanical function assessed by ballistocardiography and seismocardiography in a

- 646 context of enhanced inotropism in healthy subjects: a comparison with standard and 2D STI
 647 echocardiography. . *Submitted for publication* 2020.
- 648 36. **Moser M, Pordy L, Chesky K, Taymor RC, and Master AM.** The ballistocardiogram in
 649 myocardial infarction: a study of one hundred cases. *Circulation* 6: 402-407, 1952.
- 650 37. **Notay K, Seed JD, Incognito AV, Doherty CJ, Nardone M, Burns MJ, and Millar PJ.** Validity
 651 and reliability of measuring resting muscle sympathetic nerve activity using short sampling
 652 durations in healthy humans. *J Appl Physiol (1985)* 121: 1065-1073, 2016.
- 653 38. **O'Hare E, Flanagan D, Penzel T, Garcia C, Frohberg D, and Heneghan C.** A comparison of
 654 radio-frequency biomotion sensors and actigraphy versus polysomnography for the assessment of
 655 sleep in normal subjects. *Sleep Breath* 19: 91-98, 2015.
- 656 39. **Oikawa S, Hirakawa H, Kusakabe T, Nakashima Y, and Hayashida Y.** Autonomic
 657 cardiovascular responses to hypercapnia in conscious rats: the roles of the chemo- and
 658 baroreceptors. *Auton Neurosci* 117: 105-114, 2005.
- 659 40. **Palada I, Bakovic D, Valic Z, Obad A, Ivancev V, Eterovic D, Shoemaker JK, and Dujic Z.**
 660 Restoration of hemodynamics in apnea struggle phase in association with involuntary breathing
 661 movements. *Respir Physiol Neurobiol* 161: 174-181, 2008.
- 662 41. **Parish JM, and Somers VK.** Obstructive sleep apnea and cardiovascular disease. *Mayo Clin*
 663 *Proc* 79: 1036-1046, 2004.
- 664 42. **Penzel T, Schobel C, and Fietze I.** New technology to assess sleep apnea: wearables,
 665 smartphones, and accessories. *F1000Res* 7: 413, 2018.
- 666 43. **Pingitore A, Gemignani A, Menicucci D, Di Bella G, De Marchi D, Passera M, Bedini R,**
 667 **Ghelarducci B, and L'Abbate A.** Cardiovascular response to acute hypoxemia induced by
 668 prolonged breath holding in air. *Am J Physiol Heart Circ Physiol* 294: H449-455, 2008.
- 669 44. **Polo O, Tafti M, Hamalainen M, Vaahtoranta K, and Alihanka J.** Respiratory variation of
 670 the ballistocardiogram during increased respiratory load and voluntary central apnoea. *Eur Respir J*
 671 5: 257-262, 1992.
- 672 45. **Prabhakar NR, and Kumar GK.** Mechanisms of sympathetic activation and blood pressure
 673 elevation by intermittent hypoxia. *Respir Physiol Neurobiol* 174: 156-161, 2010.
- 674 46. **Saito M, Mano T, Iwase S, Koga K, Abe H, and Yamazaki Y.** Responses in muscle
 675 sympathetic activity to acute hypoxia in humans. *J Appl Physiol (1985)* 65: 1548-1552, 1988.
- 676 47. **Seitz MJ, Brown R, and Macefield VG.** Inhibition of augmented muscle vasoconstrictor
 677 drive following asphyxic apnoea in awake human subjects is not affected by relief of chemical
 678 drive. *Exp Physiol* 98: 405-414, 2013.
- 679 48. **Shimizu T, Takahashi Y, Kogawa S, Takahashi K, Kanbayashi T, Saito Y, and Hishikawa Y.**
 680 Muscle sympathetic nerve activity during apneic episodes in patients with obstructive sleep apnea
 681 syndrome. *Electroencephalogr Clin Neurophysiol* 93: 345-352, 1994.
- 682 49. **Somers VK, Dyken ME, Clary MP, and Abboud FM.** Sympathetic neural mechanisms in
 683 obstructive sleep apnea. *J Clin Invest* 96: 1897-1904, 1995.
- 684 50. **Somers VK, Dyken ME, and Skinner JL.** Autonomic and hemodynamic responses and
 685 interactions during the Mueller maneuver in humans. *J Auton Nerv Syst* 44: 253-259, 1993.
- 686 51. **Somers VK, Mark AL, Zavala DC, and Abboud FM.** Contrasting effects of hypoxia and
 687 hypercapnia on ventilation and sympathetic activity in humans. *J Appl Physiol (1985)* 67: 2101-
 688 2106, 1989.
- 689 52. **Starr I.** The relation of the ballistocardiogram to cardiac function. *Am J Cardiol* 2: 737-747,
 690 1958.
- 691 53. **Starr I, and Friedland CK.** On the Cause of the Respiratory Variation of the
 692 Ballistocardiogram, with a Note on Sinus Arrhythmia. *J Clin Invest* 25: 53-64, 1946.

- 693 54. **Starr I. NA.** *Ballistocardiography in Cardiovascular Research. Physical aspects of the*
694 *circulation in health and disease.* 1967.
- 695 55. **Steinback CD, Salzer D, Medeiros PJ, Kowalchuk J, and Shoemaker JK.** Hypercapnic vs.
696 hypoxic control of cardiovascular, cardiovagal, and sympathetic function. *Am J Physiol Regul Integr*
697 *Comp Physiol* 296: R402-410, 2009.
- 698 56. **Stromme SB, Kerem D, and Elsner R.** Diving bradycardia during rest and exercise and its
699 relation to physical fitness. *J Appl Physiol* 28: 614-621, 1970.
- 700 57. **Taebl A SB, Bomar AJ, Sandler RH, Mansy HA.** Recent Advance in Seismocardiography.
701 *Vibration* 2: 64-86, 2019.
- 702 58. **Tavakolian K, Portacio G, Tamddondoust NR, Jahns G, Ngai B, Dumont GA, and Blaber AP.**
703 Myocardial contractility: a seismocardiography approach. *Conf Proc IEEE Eng Med Biol Soc* 2012:
704 3801-3804, 2012.
- 705 59. **Vallbo AB.** Microneurography: how it started and how it works. *J Neurophysiol* 120: 1415-
706 1427, 2018.
- 707 60. **Van De Borne P, Montano N, Narkiewicz K, Degaute JP, Malliani A, Pagani M, and Somers**
708 **VK.** Importance of ventilation in modulating interaction between sympathetic drive and
709 cardiovascular variability. *Am J Physiol Heart Circ Physiol* 280: H722-729, 2001.
- 710 61. **van de Borne P, Montano N, Pagani M, Oren R, and Somers VK.** Absence of low-frequency
711 variability of sympathetic nerve activity in severe heart failure. *Circulation* 95: 1449-1454, 1997.
- 712 62. **van De Borne P, Neubauer J, Rahnama M, Jansens JL, Montano N, Porta A, Somers VK,**
713 **and Degaute JP.** Differential characteristics of neural circulatory control: early versus late after
714 cardiac transplantation. *Circulation* 104: 1809-1813, 2001.
- 715 63. **van de Borne P, Oren R, Anderson EA, Mark AL, and Somers VK.** Tonic chemoreflex
716 activation does not contribute to elevated muscle sympathetic nerve activity in heart failure.
717 *Circulation* 94: 1325-1328, 1996.
- 718 64. **van de Borne P, Rahnama M, Mezzetti S, Montano N, Porta A, Degaute JP, and Somers**
719 **VK.** Contrasting effects of phentolamine and nitroprusside on neural and cardiovascular variability.
720 *Am J Physiol Heart Circ Physiol* 281: H559-565, 2001.
- 721 65. **Velez-Roa S, Ciarka A, Najem B, Vachierey JL, Naeije R, and van de Borne P.** Increased
722 sympathetic nerve activity in pulmonary artery hypertension. *Circulation* 110: 1308-1312, 2004.
- 723 66. **Wehrwein EA, Orer HS, and Barman SM.** Overview of the Anatomy, Physiology, and
724 Pharmacology of the Autonomic Nervous System. *Compr Physiol* 6: 1239-1278, 2016.
- 725 67. **White DW, Shoemaker JK, and Raven PB.** Methods and considerations for the analysis and
726 standardization of assessing muscle sympathetic nerve activity in humans. *Auton Neurosci* 193: 12-
727 21, 2015.
- 728 68. **Wu H, Zhan X, Zhao M, and Wei Y.** Mean apnea-hypopnea duration (but not apnea-
729 hypopnea index) is associated with worse hypertension in patients with obstructive sleep apnea.
730 *Medicine (Baltimore)* 95: e5493, 2016.
- 731 69. **Xie A, Skatrud JB, Puleo DS, and Morgan BJ.** Exposure to hypoxia produces long-lasting
732 sympathetic activation in humans. *J Appl Physiol (1985)* 91: 1555-1562, 2001.
- 733

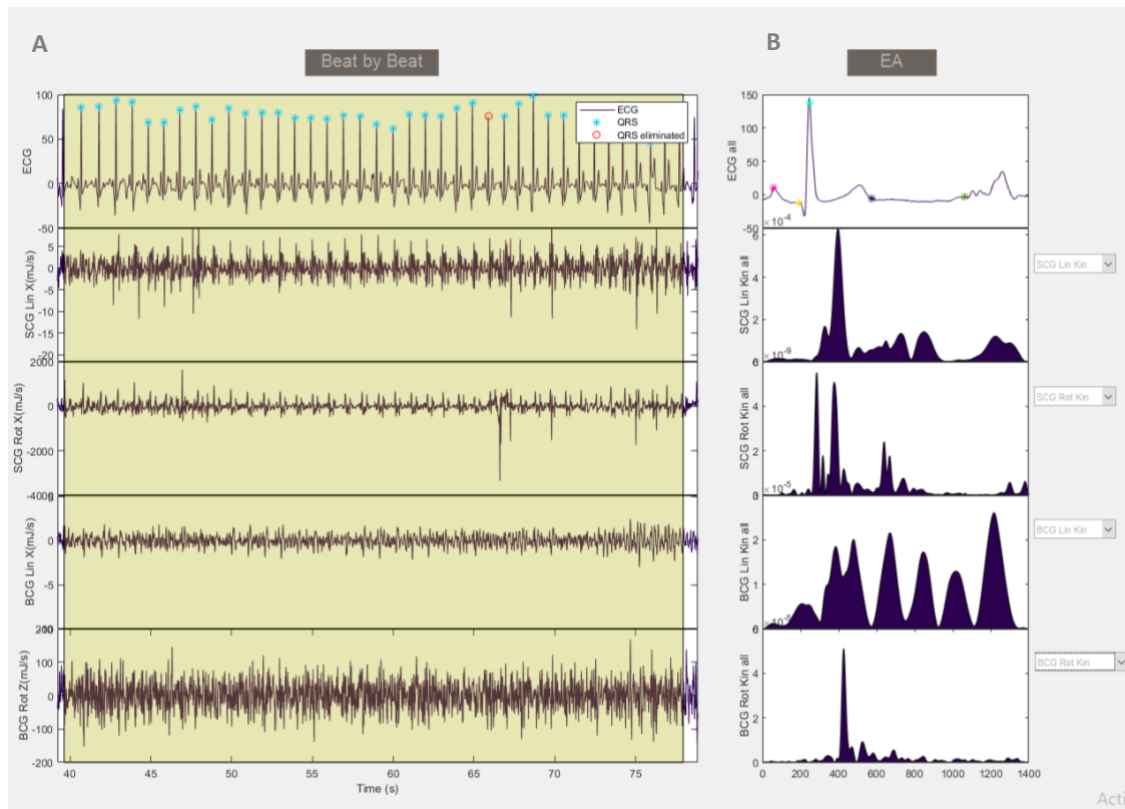


Figure 1. Toolbox written in Matlab (Mathwork® version 2019b) for the manual identification of BCG and SCG signals (panel A) and automatic computation of \mathcal{K} (panel B). Panel A: manual selection of the temporal window of consecutive beats. The beats sampled in the selected temporal region were identified based on the automatic identification of the peak ECG-R wave. From top to bottom: ECG; KE of SCG in the linear dimension; KE of SCG in the rotational dimension; KE of BCG in the linear dimension; KE of BCG in the rotational dimension. Panel B: ensemble averaging (EA) of \mathcal{K} of the selected consecutive beats over the selected temporal window. From top to bottom: EA of ECG; EA of \mathcal{K} of SCG in the linear dimension; EA of \mathcal{K} of SCG in the rotational dimension; EA of \mathcal{K} of BCG in the linear dimension; EA of \mathcal{K} of BCG in the rotational dimension. KE, kinetic energy; \mathcal{K} , integral of kinetic energy; EA, ensemble averaging; BCG, ballistocardiography; SCG sesimocardiography.

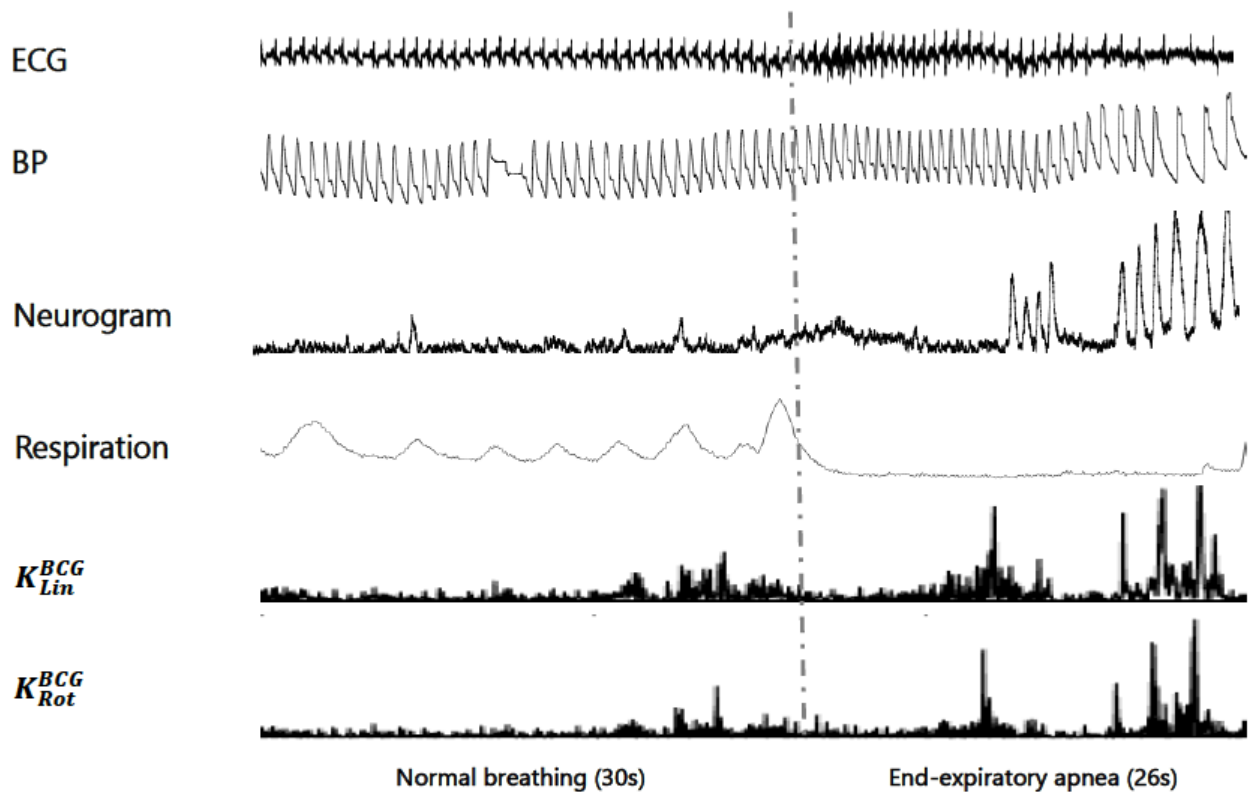
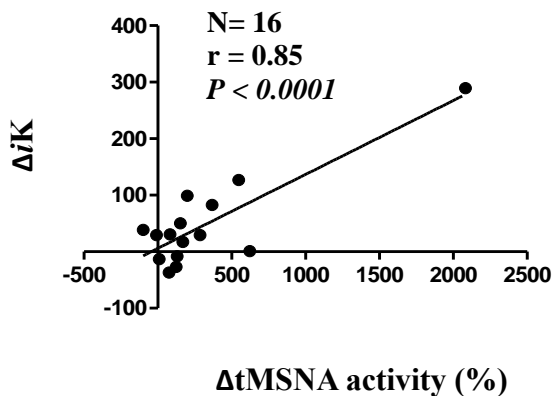


Figure 2. MSNA variations along with K_{Lin}^{BCG} and K_{Rot}^{BCG} of BCG during baseline and maximal end-expiratory voluntary apnea. Normal respiration (30s length) and maximal voluntary end-expiratory apnea (26s length) are separated by the vertical dotted grey line. From top to bottom: ECG; BP; neurogram, respiration; K_{Lin}^{BCG} ; K_{Rot}^{BCG} .

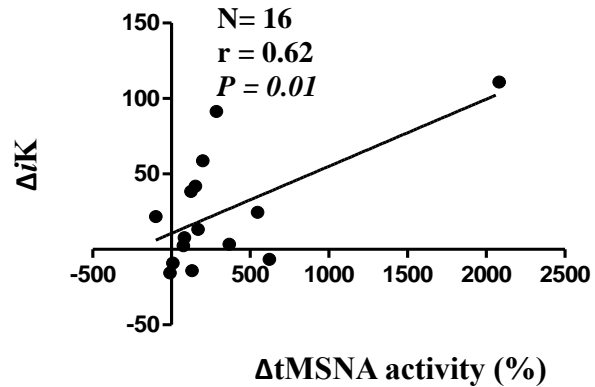
At the beginning of the apnea, there is a suppression of the sympathetic nerve activity without discernable bursts along with mild cardiac kinetic energy recorded with the BCG both in the linear and the rotational dimension. HR accelerates compared to normal respiration and systolic blood pressure slightly falls. Towards the end of the apnea, a marked rise in the sympathetic nerve activity is observed, characterized by an increase of BF and tMSNA and this is accompanied by a marked increase of linear and rotational kinetic energy. HR slows and systolic blood pressure rises compared to the beginning of the apnea.

MSNA, muscle sympathetic nerve activity; BP, blood pressure; HR, heart rate; K_{Lin} , kinetic energy in the linear dimension; K_{Rot} , integral of kinetic energy in the rotational dimension; BF, burst frequency (burst/min); tMSNA, total muscle sympathetic nerve activity; BCG, ballistocardiography.

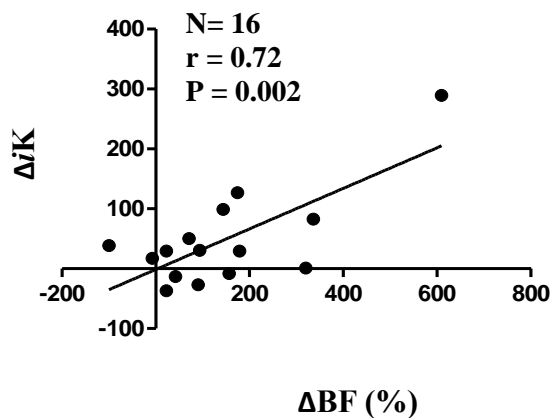
A. ΔiK_{Lin} of BCG vs $\Delta tMSNA$



B. ΔiK_{Lin} of SCG vs $\Delta tMSNA$ activity



C. ΔiK_{Lin} of BCG vs ΔBF



D. ΔiK_{Lin} of SCG vs ΔBF

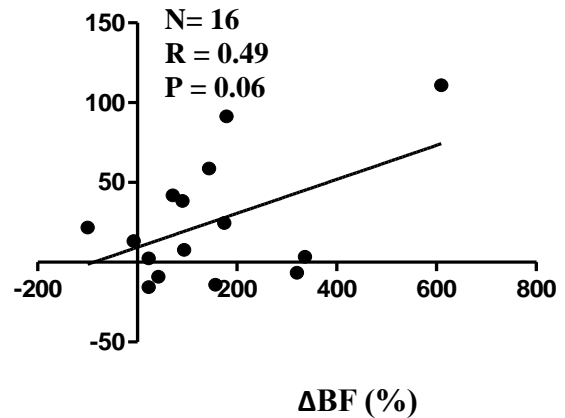


Figure 3. Correlation between ΔK (%) of BCG and SCG and $\Delta tMSNA$ (%). Δ is the difference between BSL and the last third of the apnea. A) Correlation of ΔK_{Lin} of BCG and $\Delta tMSNA$ activity ; B) Correlation of ΔK_{Lin} of SCG and $\Delta tMSNA$ activity ; C) ΔK_{Lin} of BCG and ΔBF ; D) ΔK_{Lin} of SCG and ΔBF .

The point with the highest tMSNA value is not an outlier and corresponds to a subject which presented a striking rise in MSNA during the apnea. It has been calculated a BF of 48.3 burst/min and a mean burst amplitude of 6.74 AU during the last third of the apnea (tMSNA=325.5 AU/min), compared to the BSL, where the BF was of 6.8 burst/min and the mean burst amplitude of 2.1 AU (tMSNA=14.9 AU/min). MSNA activity, along with cardiac kinetic energy, for this subject is shown in figure 2.

BCG, ballistocardiography ; BF, burst frequency ; K_{Lin} , linear kinetic energy ; tMSNA, total muscular sympathetic nerve activity.

Table 1. Modifications of hemodynamic parameters along with metrics of MSNA activity during the baseline and the apnea.			
Parameter	Baseline	Apnea	p-value
SBP (mmHg)	115 ± 11	120 ± 12	0.01
DBP (mmHg)	59 ± 9	61 ± 11	0.1
MBP (mmHg)	79 ± 10	82 ± 13	0.1
HR (bpm)	65 ± 7	67 ± 11	0.2
SatO₂ (%)	97 ± 2	96 ± 4	0.02
ETCO₂ (mmHg)	40 ± 3	42 ± 5	0.1
BF (burst/min)	18.9 ± 9.9	28.4 ± 10.6	0.002
tMSNA (AU/min)	46.7 [28.8; 63.8]	84.0 [59.9; 184.5]	0.001
SBP, systolic blood pressure (mmHg); DBP, diastolic blood pressure (mmHg); MBP, mean blood pressure (mmHg); PP, pulse pressure (mmHg); HR, heart rate (bpm); SatO ₂ , oxygen saturation (%); ETCO ₂ , end-tidal CO (mmHg); BF, burst frequency (burst/min); tMSNA, total MSNA activity (AU/min). Data are presented as mean ± SD or median [P25; P75] according to data distribution.			

Table 2. Modifications of metrics of MSNA activity, K of SCG and BCG from baseline to the end of the apnea.

Parameters	Baseline	1/3 apnea	2/3 apnea	3/3 apnea	p_{ALL}
BF (burst/min)	18.9 ± 9.9	23.9 ± 21.7	26.2 ± 16.2	37.3 ± 18.0	0.02
tMSNA (AU/min)	46.7 [28.8; 63,8]	57.8 [10.6; 137.9]	76.5 [30.5; 182.3]	128.7 [70.3; 308.5]	0.01
iK_{Lin}^{SCG} (μJ.s)	100 [80; 100]	100 [60; 180]	110[70; 190]	110[80; 190]	0.46
iK_{Rot}^{SCG} (nJ.s)	0.9 [0.5; 1.3]	0.9 [0.5; 1.3]	1.1 [0.6; 1.8]	1.1 [0.4; 1.9]	0.12
iK_{Lin}^{BCG} (μJ.s)	7.6 [5.5; 12.5]	8.8 [7.0; 1400]	200 [6.7; 1600]	9.3 [6.5; 1500]	0.03
iK_{Rot}^{BCG} (μJ.s)	2.9 [1.5; 4.5]	3.6 [3.0; 4.7]	3.4 [2.9; 5.3]	3.3 [2.9; 5.2]	0.0005

BF, burst frequency (burst/min); tMSNA, total MSNA activity (AU/min);

iK_{Lin}^{SCG} (μJ.s) and iK_{Rot}^{SCG} (nJ.s), integral of kinetic energy of the SCG in the linear and rotational dimension, respectively;

iK_{Lin}^{BCG} (μJ.s) and iK_{Rot}^{BCG} (μJ.s) integral of kinetic energy of the BCG in the linear and rotational dimension, respectively;

Data are presented as mean ± SD or median and [P25; P75] according to data distribution.

Table 3. Correlation analysis of ΔiK of BCG and SCG with ΔBF and $\Delta tMSNA$ for each epoch of apnea.

<i>N</i> = 16	ΔiK_{Lin} BCG	ΔiK_{Rot} BCG	ΔiK_{Lin} SCG	ΔiK_{Rot} SCG
<i>BSL and 1/3 apnea</i>				
$\Delta tMSNA$	$r = 0.13, p = 0.65$	$r = 0.009, p = 0.94$	$r = -0.02, p = 0.95$	$r = -0.06, p = 0.83$
ΔBF	$r = -0.003, p = 0.97$	$r = 0.01, p = 0.97$	$r = -0.13, p = 0.65$	$r = 0.008, p = 0.98$
<i>BSL and 2/3 apnea</i>				
$\Delta tMSNA$	$r = 0.45, p = 0.055$	$r = 0.09, p = 0.73$	$r = 0.44, p = 0.09^*$	$r = -0.25, p = 0.34^*$
ΔBF	$r = 0.52, p = 0.04$	$r = 0.18, p = 0.52$	$r = 0.51, p = 0.04^*$	$r = -0.22, p = 0.41^*$
<i>BSL and 3/3 apnea</i>				
$\Delta tMSNA$	$r = 0.85, p < 0.0001$	$r = -0.17, p = 0.95$	$r = 0.62, p = 0.01$	$r = 0.06, p = 0.08$
ΔBF	$r = 0.72, p = 0.002$	$r = -0.03, p = 0.93$	$r = 0.49, p = 0.06$	$r = 0.14, p = 0.62$

Pearson's correlation of ΔiK (%) of BCG and SCG with $\Delta tMSNA$ and ΔBF (%). The differences (Δ) between: BSL and the 1/3 of apnea; BSL and the 2/3 of apnea; BSL and the 3/3 of apnea have been normalized for the BSL and are expressed in %. BCG, ballistocardiography; SCG, seismocardiography; BF, burst frequency; iK_{Lin} and iK_{Rot} , linear and rotational kinetic energies, respectively; $tMSNA$, total muscular sympathetic nerve activity. * Spearman correlation.